

**UCLA**

**UCLA Electronic Theses and Dissertations**

**Title**

The impact of Estrogen Receptor Alpha expression on Cardiomyocellular architecture and metabolism

**Permalink**

<https://escholarship.org/uc/item/1cv1s58v>

**Author**

Strumwasser, Alexander Rahbar

**Publication Date**

2022

Peer reviewed|Thesis/dissertation

UNIVERSITY OF CALIFORNIA  
Los Angeles

The impact of Estrogen Receptor Alpha expression on Cardiomyocellular architecture and  
metabolism

A thesis submitted in partial satisfaction  
of the requirements for the degree Master of Science  
in Physiological Science

by

Alexander Rahbar Strumwasser

2022

© Copyright by  
Alexander Rahbar Strumwasser  
2022

## ABSTRACT OF THE THESIS

The impact of Estrogen Receptor Alpha expression on Cardiomyocellular architecture and  
metabolism

by

Alexander Rahbar Strumwasser

Master of Science in Physiological Science

University of California, Los Angeles, 2022

Professor Xia Yang, Co-Chair

Professor Andrea L Hevener, Co-Chair

Sex differences in the onset and manifestation of cardiovascular disease are well described, yet the mechanism(s) underlying these clinical observations remain inadequately understood. Estradiol ( $E_2$ ) exerting its effects through receptors in responsive tissues has been shown to protect the heart from cytotoxic, ischemic, and hypertrophic stressors; however, the actions of this hormone are complex and remain inadequately understood. Although the modulatory effects of  $E_2$  on vascular endothelium and the heart are well-defined, receptor mediated action on cardiomyocytes, specifically estrogen receptor alpha ( $ER\alpha$ ), lacks a mechanistic understanding and requires further resolution. Here we show that that *Esr1*, the gene that encodes  $ER\alpha$ , is crucial in the maintenance of cardiac functional capacity and is essential for mitochondrial form and function including membrane architecture, energy homeostasis, metabolic flexibility, and substrate metabolism.

The thesis of Alexander Rahbar Strumwasser is approved.

Stephanie Correa Van Veen

Mansoureh Eghbali

Xia Yang, Committee Co-Chair

Andrea L Hevener, Committee Co-Chair

University of California, Los Angeles

2022

## DEDICATION

I dedicate this thesis to all of those who have guided me throughout this process. To Tash, Scott, and Roxanna Strumwasser; you have cultivated for me a life full of curiosity and opportunity. Thank you for your limitless support. To my friends, colleagues, and mentors at UCLA these works are for you - Dr. Andrea Hevener, Dr. Zhenqi Zhou and Dr. Timothy M. Moore; your guidance and wisdoms will never be forgotten. Finally, to Whitney Nelson; without you, the future would not be as bright.

## TABLE OF CONTENTS

Abstract .....	ii
Dedication .....	iv
List of figures .....	vi
Introduction .....	1
Materials and methods .....	5
Results .....	11
Discussion .....	19
Conclusion .....	23
References .....	25

## LIST OF FIGURES

<b>Figure 1:</b> Protein and gene expression levels of estrogen receptor alpha after cardiomyocyte specific knock-down and survival curve of homozygous knock-down model.....	12
<b>Figure 2:</b> Functional analysis of echocardiogram from female hER $\alpha$ <sup>KD</sup> and controls at three time points, mRNA expression levels from whole hear tissue, and histological analysis of Masson’s trichrome stain.....	13
<b>Figure 3:</b> Transmission electron micrograph images, Seahorse assay and protein expression levels of OXPHOS complexes.....	15
<b>Figure 4:</b> Mitochondrial fission-fusion and apoptotic protein expression level from whole hear tissue.....	16
<b>Figure 5:</b> Volcano plot from RNA sequencing data of differentially expressed genes from whole hear tissue of hER $\alpha$ <sup>KD</sup> and control female mice.....	17
<b>Figure 6:</b> Metabolomics analysis from whole hear tissue of hER $\alpha$ <sup>KD</sup> and control female mice.....	18
<b>Figure 7:</b> Bioinformatic and pathway analysis of differentially expressed genes from RNA sequencing data.....	19



## **INTRODUCTION**

Each year cardiovascular diseases (CVDs) affect more than 22 million people annually, making them the number one source of morbidity and mortality worldwide<sup>1-3</sup>. More commonly allied with the accumulation of “fatty” deposits within arteries leading to atherosclerosis and an increased risk of blood clots, CVDs also involve chronic pathologies or acute injury to structures like the brain, lungs, kidney, and heart. The most well-known CVDs are coronary artery disease, myocardial infarction, arrhythmias, and heart failure (HF).

There are more than 6 million Americans living with heart failure (HF) and according to the American Heart Association over 900,000 new diagnoses each year<sup>4-6</sup>. Patients with HF take on average six HF-related medications, and 78 percent have at least two hospital admissions per year, amounting to billions of dollars in annual cost. By the age of 40, one in five Americans will have a chance of developing HF, and by 65, 10 in every 1000 people will be diagnosed with chronic progressive heart failure<sup>8</sup>. Epidemiological studies suggest that African Americans have the highest occurrence of HF, followed by Hispanic, Caucasian, and Asian Americans with an incidence rate of 4.6, 3.4, 2.4, and 1.0 percent per 1000 people, respectively<sup>9</sup>. Furthermore, HF has been identified as more common in males than females until the age of 65 when the prevalence becomes equal among both sexes<sup>9-12</sup>.

Sex as an independent risk factor is gaining support among the scientific community as a profound prognostic factor in the outcome of patients diagnosed with heart failure. Clinical studies indicate that premenopausal women have reduced incidence of CVD, including heart failure, compared to age-matched men<sup>10,11</sup>. This observation has led to

the notion that Estradiol ( $E_2$ ), working via its receptors, may be cardioprotective, a conclusion supported by numerous controlled preclinical studies. However, trials testing the role of  $E_2$  hormone replacement therapy (HRT) as a preventive measure have yielded mixed results, with the Women's Health Initiative (WHI) and Heart and Estrogen/progestin Replacement Study (HERS), showing no overall benefit<sup>13,14</sup>. The discrepancy between the initial findings of these trials and the cardioprotection by estrogen seen in experimental models is an intricate issue that requires a thorough and rigorous interrogation.

Early menopause is associated with increased risk of incidence of HF [OR 1.66 (1.01-2.73)]. Whereas increased age at menopause is associated with decreased risk of incident HF [OR 0.96 (0.94-0.99)]<sup>18,19</sup>. More recently, ESR1 (gene encoding for estrogen receptor alpha) was shown to be a top gene hub predictive of HF in the GSE dataset of over 350 patient samples<sup>17</sup>. These observations have led to the view that  $E_2$  action mediated by receptor-specific binding, may be cardioprotective against cytotoxic, ischemic, and hypertrophic stressors<sup>20-24</sup>.  $E_2$  is the most common form of circulating estrogen as well as the major female sex hormone, exerting its effects through both genomic and non-genomic actions, modulating cardiovascular physiology predominantly by binding to the estrogen receptors estrogen receptor-alpha  $ER\alpha$ , estrogen receptor-beta and ( $ER\beta$ ) and G-protein-coupled ER (GPR30)<sup>25</sup>.  $ER\alpha$  has an elevated tissue expression, strong binding efficacy and a robust gene signature shown to protect against dilated cardiomyopathy and ischemia-reperfusion injury (IRI).  $ER\alpha$  binds to chromatin as dimers at specific DNA sequences known as estrogen response elements (EREs); or may activate other transcription factors to regulate downstream gene expression<sup>26,27</sup>. Although

the protective effects of E<sub>2</sub> against HF by regulating functional capacity, cardiac fibrosis, oxidative stress, mitochondrial function, and hypertrophy have been studied, the selective effects of ER $\alpha$  in the regulation of E<sub>2</sub> mediated outcomes are less understood.

From a functional standpoint, HF describes a complex pathology in which the heart loses the ability to maintain a cardiac output (CO) sufficient to sustain metabolic demand and accommodate venous return. CO is defined as the amount of blood pumped out of the heart over a given period. Although, there are many etiologies of HF, some tend to more adversely affect either systolic (70% of patients) or diastolic function (30% of patients)<sup>28-30</sup>. Whether or not a patient with HF has systolic or diastolic dysfunction depends on the ejection fraction (EF), which is defined as the amount of blood pumped from the ventricle in one heartbeat. If the EF is less than 45%, it is considered systolic dysfunction. In systolic failure, the reduced ejection fraction is the result of an inadequate contractile force to expel requisite amount of blood into circulation<sup>31</sup>. This is also known as heart failure with reduced ejection fraction (HFrEF). Diastolic failure, or heart failure with preserved ejection fraction (HFpEF) occurs when the left ventricle loses its ability to relax due to increased muscle rigidity<sup>32</sup>. That rigidity impedes the heart's ability to fill with deoxygenated blood during the resting period between each heart contraction. Epidemiological data demonstrates that women are about twice as likely to develop HFpEF as compared to men and that they tend to present with significant comorbidities, including increased diastolic dysfunction and enhanced left ventricle stiffness<sup>32</sup>.

Cardiometabolic dysfunction leading to a deleterious reduction in functional myocardial cells is gaining traction in the literature as a possible cause or comorbidity of heart failure. Some studies suggest heart failure is accompanied by derangements in mitochondrial

function including ATP production, ROS production, calcium, and iron handling, as well as mitochondrial architecture and quality control<sup>33</sup>. On average the human heart consumes 8-13 mL•100 g<sup>-1</sup>•min<sup>-1</sup> of oxygen to oxidize substrates fueling the contracting heart<sup>34</sup>. To maintain the constant work performed by heart, cardiomyocytes must continuously consume large amounts of energy/ATP supplied by mitochondrial oxidative phosphorylation (95% of cellular energy demand). Although the mitochondrion is known as the powerhouse of the cell, it is critically involved in regulating other processes including calcium and iron homeostasis, cholesterol and steroidogenesis, and stress signaling<sup>18</sup>. Under normal conditions, the cardiomyocyte relies predominantly of fatty acids as a substrate (60-90%) with glucose providing much of the remaining fuel contribution. When necessary, the heart can also rely on ketone bodies as a primary substrate. Interestingly cardiomyocytes switch to this fuel source under failing conditions<sup>33,36-39</sup>. The mechanisms underlying the drive for ketone oxidation during heart failure require further resolution.

As a high energy demand organ, the heart consumes ATP derived from mitochondria, organelles that occupy approximately one-third of adult cardiomyocytes by volume. Moreover, mitochondria are highly dynamic organelles whose morphology is rapidly regulated by fission and fusion events in response to environmental and metabolic stress. We find in other metabolic tissues that *Esr1* exerts strong regulatory control over mitochondrial dynamics. Our studies on mitochondrial fission in skeletal muscle show that the fission regulatory protein dynamin related protein (Drp) 1 is critical for cristae formation and the assembly of the TCA/electron transport chain. Drp1 expression is also

essential for fatty acid oxidation, and thus a striking feature of muscle cells harboring dysfunctional or reduced Drp1 is disruption of lipid metabolism<sup>40-43</sup>.

Given that menopause is associated with diminished estrogen action in metabolic tissues, the extensive evidence for the role of mitochondria in heart failure and because HF is of increasing concern in women's health, the purpose of my thesis was to leverage novel mouse models and research tools to interrogate molecular actions of ER $\alpha$  on mitochondrial function in cardiomyocytes. We hypothesize that the cardioprotective effects of E<sub>2</sub> mediated by ER $\alpha$  is vital for the homeostatic maintenance of cardiac function, and is essential for membrane architecture, energy homeostasis, metabolic flexibility and substrate metabolism of mitochondria within cardiomyocytes.

## **METHODS AND MATERIALS**

### ***Ethical Approval***

This study was approved by the University of California, Los Angeles Institutional Animal Care and Use Committee. All animal care, maintenance, surgeries, and euthanasia were conducted in accordance with this Institutional Animal Care and Use Committee and the National Institute of Health.

### ***Immunoblot analysis***

Whole heart muscle was pulverized into a powder while frozen in liquid nitrogen and a homogenous sample of pulverized tissue was used for immunoblotting. Proteins from

each individual whole cell homogenate were normalized (expressed relative to the pixel densitometry) to glyceraldehyde 3-phosphate dehydrogenase, (GAPDH, AM4300, Ambion) or heat shock protein family-40 (Hsp40, ab223607). Primary antibodies included: Mitochondrial Fission Protein 1 (Fis1, GTX111010, GeneTex), Mitochondrial fission factor (MFF, ab81127, Abcam), Mitofusin 1 (MFN1, 75-162, NeuroMab), Mitofusin2 (MFN2, ab56889, Abcam), Dynamin-related protein 1 (Drp1, 8570, Cell Signaling), OxPhos Complex I to V (ab110413, Abcam), Optic atrophy 1 (Opa1, 612606, BD Biosciences), Parkin (2132, Cell Signaling), Microtubule-associated proteins 1A/1B light chain 3B (LC3B, 2775, Cell Signaling), Sequestosome 1 (p62, 5114, Cell Signaling).

#### ***DNA & RNA extraction, cDNA synthesis, quantitative RT-PCR***

DNA and RNA were extracted from a homogenous portion of frozen heart tissue using DNeasy/RNeasy Isolation kits (Qiagen) as described by the manufacturer. Isolated DNA and RNA was tested for concentration and purity using a NanoDrop Spectrophotometer (Thermo Scientific). Isolated RNA was converted into cDNA, checked for purity, and qPCR of the resulting cDNA levels was performed as previously described. All genes were normalized to the housekeeping gene Ppia or 18S.

#### ***Trans-thoracic echocardiography***

The mice were anesthetized and maintained with 1–2% isoflurane in 95% oxygen. Trans-thoracic echocardiography was conducted with Vevo 2100 high-frequency, high-resolution digital imaging system (VisualSonics) equipped with a MS400 MicroScan

Transducer. A parasternal short axis view was used to obtain M-mode images for analysis of fractional shortening, ejection fraction, and other cardiac functional parameters. The apical four-chamber view was used to obtain tissue Doppler imaging (TDI) mode and Pulse-wave Doppler (PWD) mode for analysis of myocardial velocity and blood flow velocity, respectively.

### ***Tissue histology***

Heart tissue from both control and hER $\alpha$ <sup>KD</sup> female mice were sectioned and stained for hematoxylin and eosin or cytochrome c oxidase (COX) as previously described. Muscle fiber area, nuclei number, and fiber number were counted or measured using ImageJ software.

### ***RNA Isolation, Library Preparation, and Sequencing***

Whole hearts were pulverized at the temperature of liquid nitrogen. Tissue was homogenized in Trizol (Invitrogen, Carlsbad, CA, USA), RNA was isolated using the RNeasy Isolation Kit (Qiagen, Hilden, Germany), and then tested for concentration and quality with samples where RIN > 7.0 used in downstream applications. Libraries were prepared using KAPA mRNA HyperPrep Kits and KAPA Dual Index Adapters (Roche, Basel, Switzerland) per manufacturer's instructions. A total of 800-1000 ng of RNA was used for library preparation with settings 200-300 bp and 12 PCR cycles. The resultant libraries were tested for quality. Individual libraries were pooled and sequenced using a HiSeq 3000 or NovaSeq 6000 S4 UCLA Technology Center for Genomics and Bioinformatics (TCGB) following in house established protocols.

### ***Transmission Electron Microscopy (TEM)***

Heart tissue was quickly and carefully excised from the thoracic cavity. The tissue was examined for any remaining non-cardiac tissue and removed if present, then immersed in freshly prepared fixative containing 2.5% glutaraldehyde and 2% paraformaldehyde in 0.15 M cacodylate buffer and stored at 4°C until use. This fixative has been shown to preserve tissue architecture. After fixation, muscles were processed for TEM analysis as described previously (Zhou et al., 2018). Ultrathin (~60 nm) sections were viewed using a JEOL 1200EX II (JEOL, Peabody, MA, United States) electron microscope and photographed using a Gatan digital camera (Gatan, Pleasanton, CA, United States) as previously described. Mitochondrial area, perimeter, Feret's diameter, and cristae numbers were analyzed and quantified in all images by three separate and blinded individuals using ImageJ (NIH).

### ***Mitochondrial respiration***

Mitochondrial respiration was measured in frozen biological samples as described previously (Acin-Perez et al., 2020). Frozen tissues were thawed on ice and homogenized in MAS (70 mM sucrose, 220 mM mannitol, 5 mM KH<sub>2</sub>PO<sub>4</sub>, 5 mM MgCl<sub>2</sub>, 1 mM EGTA, 2 mM HEPES, pH 7.4). The samples were mechanically homogenized for 60 strokes in a Teflon-glass dounce homogenizer. All homogenates were centrifuged at 1000×g for 10 min at 4°C and then the supernatant was collected. Protein concentration was determined by BCA (Thermo Scientific). Homogenates were loaded into Seahorse XF96 microplate in 20 µl of MAS at 6 µg/well. The loaded plate was centrifuged at 2400×g for 10 min at 4°C (no brake) and an additional 130 µl of MAS supplemented with 100 µg/ml cytochrome



c was added to each well. Substrate injection was as follows: Port A: NADH (1 mM) or succinate + rotenone (5 mM + 2  $\mu$ M); Port B: rotenone + antimycin A (2  $\mu$ M + 2  $\mu$ M); Port C: N,N,N',N'-tetramethyl-p-phenylenediamine (TMPD) + ascorbic acid (0.5 mM + 1 mM); and Port D: azide (50 mM). These conditions allow for the determination of the maximal respiratory capacity of mitochondria through Complex I, Complex II, and Complex IV.

### ***Mitochondrial isolation & Metabolomic analysis***

Mitochondria were isolated from heart tissue muscle using a Dounce homogenizer and Mitochondria Isolation Kit for Tissue (Thermo Scientific) with a Percoll density method for added purification. Briefly, heart tissues were washed in ice-cold PBS, Dounce homogenized, and centrifuged at 800g for 10 min at 4°C. The supernatant was centrifuged at 12,000g for 15 min at 4°C. The pellet was washed and purified using isolation buffer and Percoll solution. Isolated mitochondria were mixed with lysis buffer (200  $\mu$ L, 12 mM sodium lauroyl sarcosine, 0.5% sodium deoxycholate, 50 mmol/L triethylammonium bicarbonate (TEAB)), then subjected to bath sonication for 10 min (Bioruptor Pico, Diagenode Inc., Denville, NJ, USA) and heated (95°C for 5 min). An aliquot of the resulting solution was assayed for total protein concentration (bicinchoninic acid assay; Micro BCA Protein Assay Kit, Thermo Fisher Scientific, Waltham, MA). The remaining samples were diluted to 0.5 mg protein/mL with lysis buffer, and an aliquot of each was mixed with tris(2-carboxyethyl) phosphine, followed by addition of chloroacetamide, diluted 5-fold with aqueous 50 mmol/L TEAB, and incubated overnight with Sequencing Grade Modified Trypsin (Promega, Madison, WI) following which an equal volume of ethyl acetate/trifluoroacetic acid. Supernatants were discarded after

centrifugation and resulting phase was vacuum dried. The samples were then desalted and loaded onto a small portion of a C18-silica disk (3M, Maplewood, MN). Prior to sample loading the C18 disk was prepared by sequential flushing with methanol, acetonitrile/water/TFA, and solvent A. The disc and sample were washed with solvent A and eluted with solvent B. The collected eluent was dried in a centrifugal vacuum concentrator and the samples were then chemically modified using a TMT10plex Isobaric Label Reagent Set (Thermo Fisher Scientific) as per the manufacturer's protocol. The TMT-labeled peptides were dried and reconstituted in solvent A, and an aliquot was taken for measurement of total peptide concentration (Pierce Quantitative Colorimetric Peptide, Thermo Fisher Scientific). The samples were then pooled according to protein content and desalted. The dried multiplexed pooled sample was reconstituted in water/acetonitrile with 10mM ammonium bicarbonate prior to fractionation via high pH reversed-phase chromatography using a 1260 Infinity LC System (Agilent Technologies, Santa Clara, CA) and a ZORBAX 300 Extend-C18 column (Agilent Technologies, 0.3 x 150 mm, 3.5  $\mu$ m) equilibrated in solvent C and eluted with an increasing concentration of solvent D. The fractions were eluted into a 96-well plate with 5% formic acid (FA) in each well over the course of 68 min. The 96 fractions were then condensed into 12 fractions prior to another desalting. The eluants were dried and reconstituted in water/acetonitrile/FA, and aliquots were injected onto a reverse phase nanobore HPLC column (AcuTech Scientific) using an Eksigent NanoLC-2D system (Sciex, Framingham, MA). The effluent from the column was directed to a nanospray ionization source connected to a hybrid quadrupole-Orbitrap mass spectrometer (Q Exactive Plus, Thermo Fisher Scientific) acquiring mass spectra in a data-dependent mode alternating between a full scan ( $m/z$  350-1700, automated gain

control (AGC) target  $3 \times 10^6$ , 50 ms maximum injection time, FWHM resolution 70,000 at  $m/z$  200) and up to 10 MS/MS scans (quadrupole isolation of charge states  $\geq 2$ , isolation width 1.2 Th) with previously optimized fragmentation conditions (normalized collision energy of 32, dynamic exclusion of 30 s, AGC target  $1 \times 10^5$ , 100 ms maximum injection time, FWHM resolution 35,000 at  $m/z$  200). The raw data was analyzed in Proteome Discoverer 2.2, providing measurements of relative abundance of the identified peptides. Uniprot was used to convert MS IDs to protein Accession IDs. Proteins significantly altered by training were analyzed using DAVID Bioinformatics Resources 6.8 for Functional Annotation Clustering and Pathview for pathway analysis.

### ***Statistical analysis***

Values are presented as means  $\pm$  SEM and expressed relative to the respective control group. Group differences were assessed by one-way ANOVA followed by Tukey Honest Significant Difference *post hoc* test, Student's T-Test, or two-way ANOVA where appropriate. Statistical significance was established *a priori* at  $P < 0.05$  (Graph Pad Prism 7.0).

## **RESULTS**

### ***ER $\alpha$ specific deletion of cardiomyocyte***

To interrogate molecular actions of ER $\alpha$  on cardiac function and mitochondrial function we created a cardiomyocyte specific *Esr1* (ER $\alpha$ ) knock-down (KD) in 3-month-old female mice. ER $\alpha$  floxed mice were crossed with the alpha-MHC-MerCreMer ( $\alpha$ MHC-MerCreMer) transgenic mouse (Sohal DS, et al<sup>44</sup>, JAX#005657) to produce a tamoxifen

inducible-heart specific knock-down of ER $\alpha$  (hER $\alpha$ <sup>KD</sup>). Western blot and qPCR analysis conferred the efficacy of our animal model at both the gene and protein level. (**Figure 1, A and B**). This transgenic mouse has a cardiac-specific alpha-myosin heavy chain promoter ( $\alpha$ MHC or alpha-MHC; *Myh6*) directing a temporal expression of a tamoxifen-inducible Cre recombinase (MerCreMer) to juvenile and adult cardiac myocytes. Heterozygotic knock-down females (hER $\alpha$ <sup>KD</sup>), and control<sup>fl/fl</sup> were produced. For all experiments both hER $\alpha$ <sup>KD</sup> and control<sup>fl/fl</sup> mice received identical intraperitoneal injections of 0.2 ml tamoxifen for five consecutive days. Preliminary studies suggest that total knock-out (hER $\alpha$ <sup>KO</sup>) of the *Esr1* gene in cardiomyocytes confers lethality (**Figure 1C**).

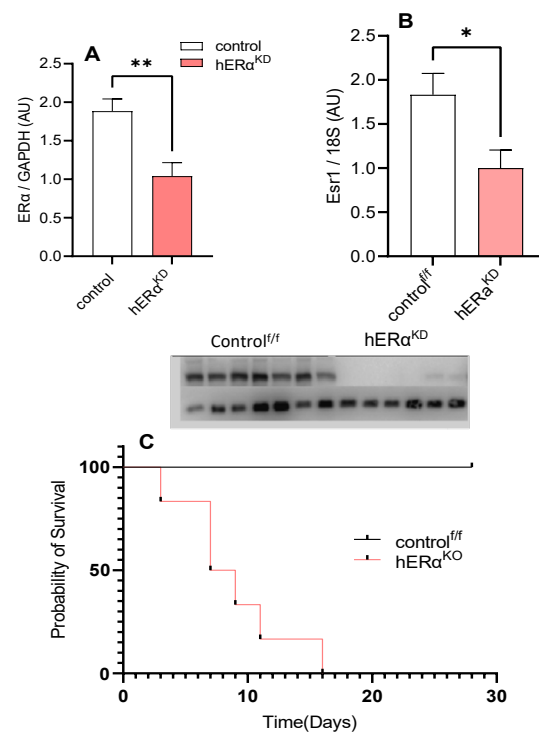


**Figure 1.** Protein (A) and mRNA expression (B) levels of female hER $\alpha$ <sup>KD</sup> vs. control<sup>fl/fl</sup> mice. Survival curve from preliminary data of total Esr1 knock-out (hER $\alpha$ <sup>KO</sup>) female mice (C).

### ***ER $\alpha$ is essential for normal cardiac function and protection against fibrosis***

To assess the cardioprotective impact of ER $\alpha$  on cardiac function we performed echocardiography on 3-month-old female hER $\alpha$ <sup>KD</sup> and control<sup>fl/fl</sup> mice. All mice were subjected to three identical echo evaluations: baseline prior to gene deletion, and 2 and

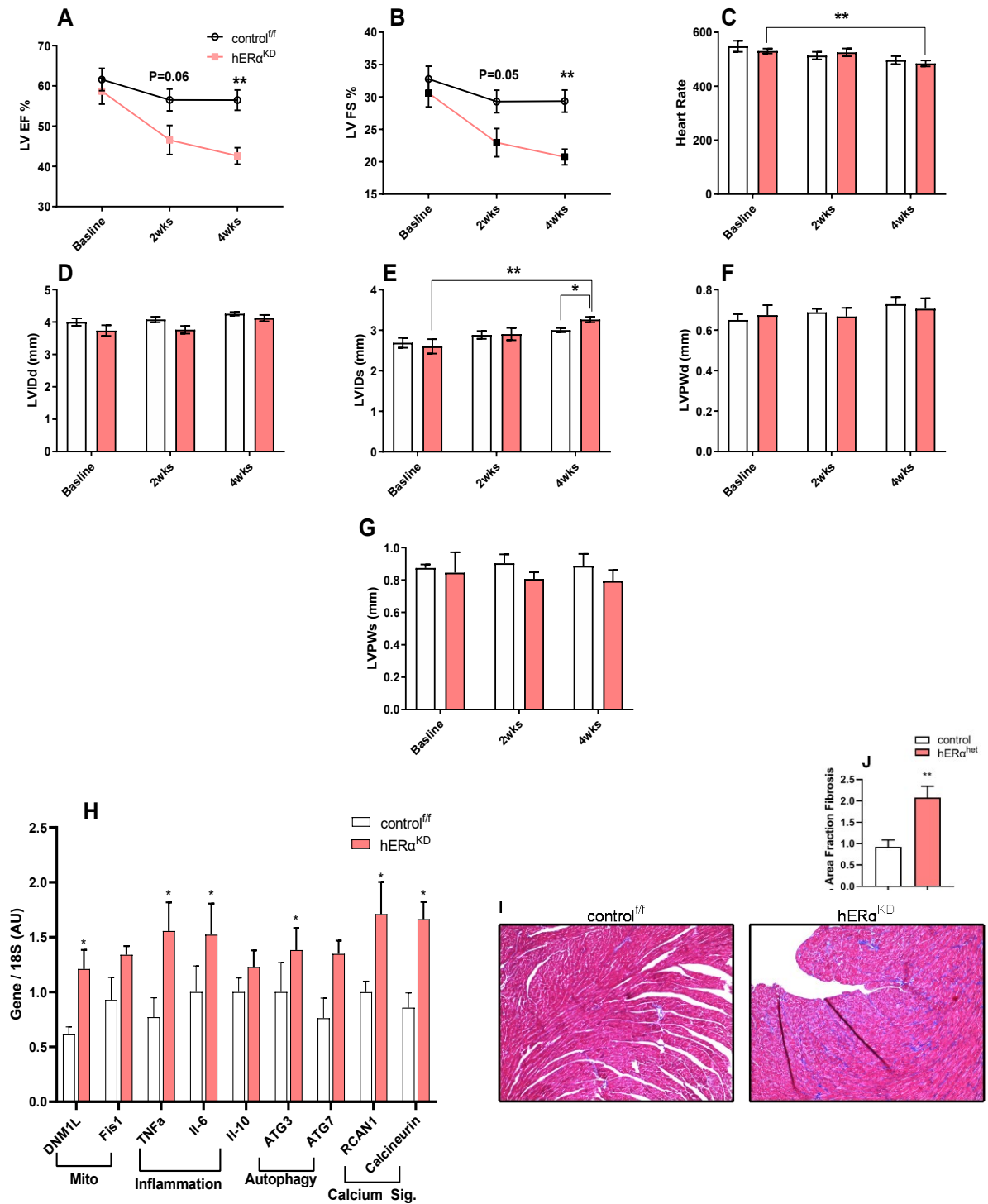


**Figure 2.** Echocardiogram analysis of left ventricular ejection fraction (EF) (**A**), left ventricular fractional shortening (FS) (**B**), heart rate (**C**), left ventricular internal diameter (LVID) during systoli (**D**) and diastoli (**E**), posterior wall thickness (LVPW) in the ventricular during systoli (**F**) and diastoli (**G**). Corresponding mRNA expression levels (**H**), Masson's Trichrome Stain (**I**) of hERA<sup>KD</sup> females vs. controls.

4-weeks after gene deletion. hER $\alpha$ <sup>KD</sup> mice presented with a reduced left ventricular ejection fraction (LVEF) reaching significance by four weeks when compared controls (**Figure 2A**). A similar finding was observed for left ventricular fractional shortening (LVFS) and heart rate (**Figure 2, B and C**). Each of these functional changes are indicative of cardiomyopathy further solidifying the significance of ER $\alpha$  in overall heart functional capacity. Previous studies have shown that E<sub>2</sub> supplementation in ovariectomized (OVX) rodents reduces cardiac fibrosis after transverse aortic constriction (TAC) and age associated fibrosis has been identified as a contributing factor to diastolic HF. Hearts from hER $\alpha$ <sup>KD</sup> and controls were harvested from 4-month-old mice, four weeks after conditional *Esr1* gene deletion with tamoxifen. Masson's trichrome staining showed a marked increase in fibrotic area in hER $\alpha$ <sup>KD</sup> compared to control<sup>fl/fl</sup> (**Figure 2, I and J**). qPCR analysis of known inflammatory genes was performed on whole-heart tissue from the same cohort, showing a marked increase in known inflammatory markers interleukin-6 (I6) and tumor necrosis factor-alpha (TNF $\alpha$ ) (**Figure 2H**).

### **ER $\alpha$ modulates mitochondrial form and energy production**

We find in all *Esr1* models we have studied to date, marked alterations in mitochondrial form and function are seen. To assess mitochondrial membrane architecture, we performed transmission electron microscopy on female hER $\alpha$ <sup>KD</sup> and control mice (**Figure 3A**). Analysis with ImageJ indicates a significant reduction in total percent area fraction (**Figure 3C**) of cristae per mitochondria, as well as the number of cristae per mitochondria (**Figure 3D**) in hER $\alpha$ <sup>KD</sup> when compared to controls. Interestingly, we show no differences in total area of mitochondria between groups (**Figure 3B**). Western blot analysis indicates

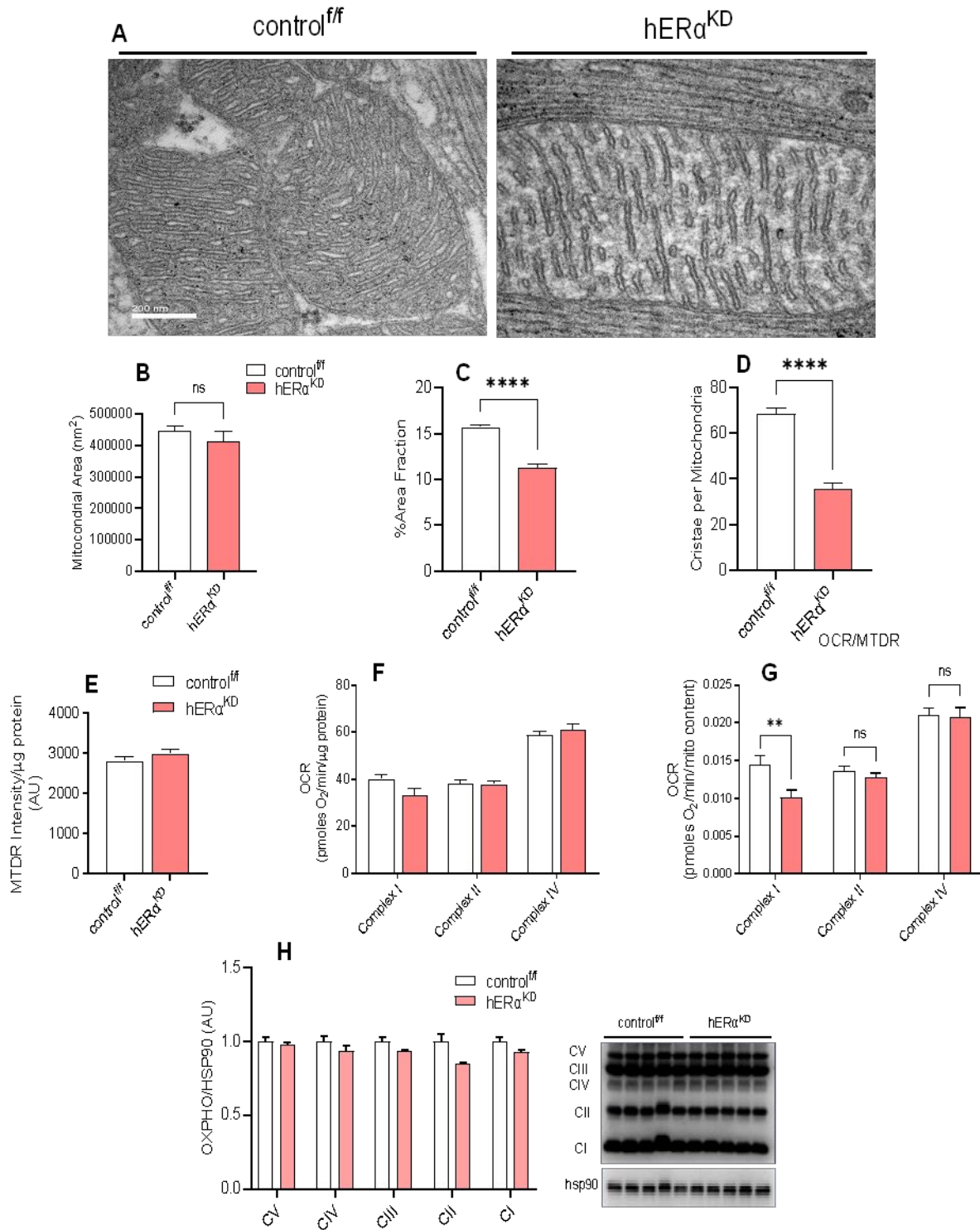


**Figure 3** Electron micrograph images (**A**), total mitochondrial area (**B**), percent area fraction of mitochondria, percent area fraction of cristae per mitochondria (**C**), total number of cristae per mitochondria (**D**), MTDR intensity per  $\mu$ g of protein (**E**), oxygen consumption rate (**F**), oxygen consumption rate as a function of MTDR (**G**) and OXPHOS protein expression levels (**H**) of hER $\alpha$ <sup>KD</sup> vs. control females

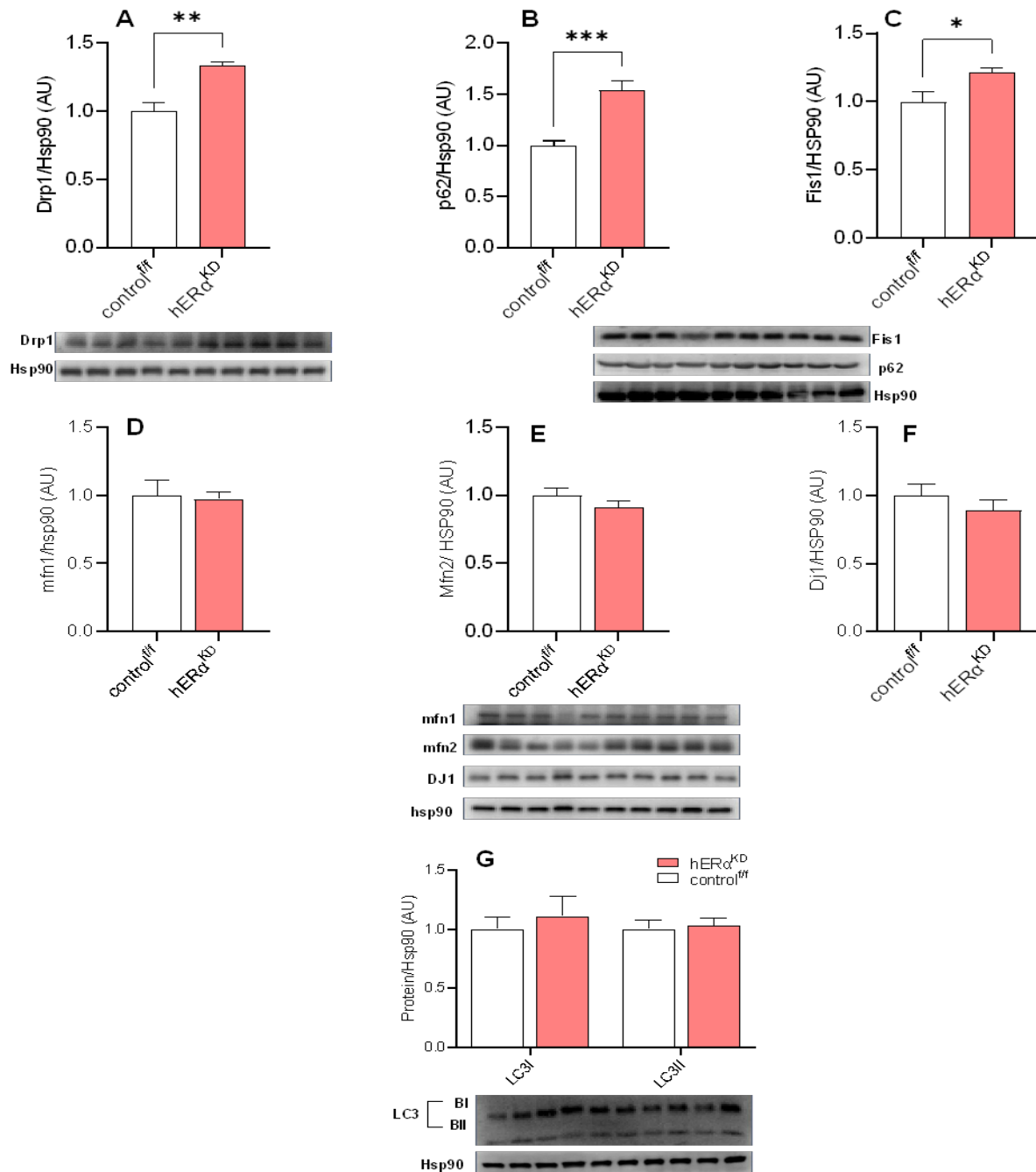


**Figure 4** Densitometry analysis of protein expression levels for hER $\alpha$ <sup>KD</sup> female mice vs. control 4 weeks after tamoxifen injection.

significant increases in protein level expression of p62, Drp1 and Fis1 (**Figure 4A-C**).

Where p62 is a known regulatory of autophagy, Drp1 and Fis1 are involved in mitochondrial dynamics and turnover, primarily fission and lipid metabolism. No



significant changes were seen in any other proteins commonly assessed by our lab (LC3, mfn1, mfn2 or Dj1) (**Figure 4D-G**). To further explore the effects of ER $\alpha$  deletion on mitochondrial function, specifically ATP synthesis and the respiratory chain complexes, Seahorse-assays were performed on frozen heart tissue<sup>45</sup>. Analysis showed that complex I activity in hER $\alpha$ <sup>KD</sup> female mice was significantly reduced when compared to that of controls (**Figure 3E-G**). Interestingly, western blot analysis shows no change in protein expression levels of any of the complexes in respiratory chain (**Figure 3H**).

### ER $\alpha$ influences cardiomyocellular metabolism

Under normal conditions, the cardiomyocyte relies predominantly of fatty acids as a substrate (60-90%) with glucose providing much of the remaining fuel contribution. When necessary, the heart can also rely on ketone bodies as a primary substrate. Interestingly cardiomyocytes

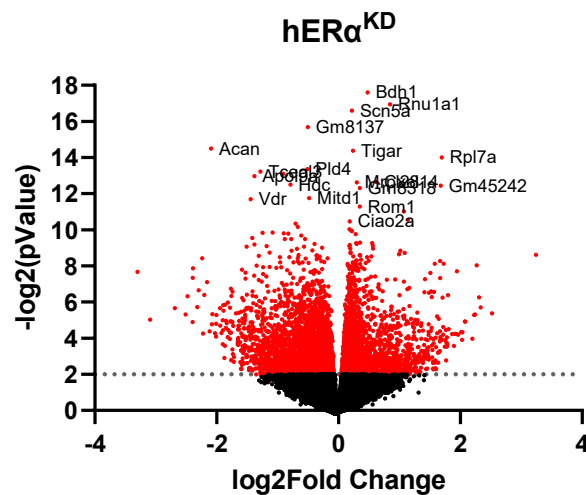


**Figure 5A** Volcano plot from RNAseq data of differentially expressed genes from hER $\alpha$ <sup>KD</sup> female mice vs. control 4 weeks after *Esr1* deletion

switch to this fuel source under failing conditions although the mechanisms underlying the drive for ketone oxidation during heart failure require further resolution. To identify whether ER $\alpha$  is also implicated in changes of mitochondrial metabolism, Metabolomics

was performed on whole heart tissue of hER $\alpha$ <sup>KD</sup> and control females. Preliminary analysis indicates alterations in methionine, pyruvate, and medium and long chain fatty acyl carnitine metabolism (Figure 6).

Methionine, Cysteine, SAM and Taurine Metabolism	methionine	0.91	Long Chain Rejuvenated Fatty Acid (n6 and n6)	tridecanoate (14:2)	1.00
	S-methylmethionine	1.01		tridecanoate (16:3n3)	1.00
	methionine sulfone	0.74		tridecanoate (18:4n3)	1.02
	N-acetylmethionine sulfide	0.90		tridecanoate (DPA, 20:5n3)	1.02
	S-adenosylmethionine (SAM)	0.98		tridecanoate (21:5n3)	0.99
	S-methylcysteine	1.03		tridecanoate (n3 DPA, 22:5n3)	0.93
Glutathione Metabolism	cysteine $\alpha$ -sulfate	1.06	tridecanoate (DPA, 22n3)	0.91	
	cystathione sulfonic acid	0.71	tridecanoate (24:5n3)	0.78	
	glutathione, reduced (GSH)	0.94	tridecanoate (26:4n3)	0.92	
	glutathione, oxidized (GSSG)	0.96	tridecanoate (22:3n3)	0.70	
	cystathionine-glutathione disulfide	0.88	tridecanoate (26)	0.94	
	2-hydroxybutyrate/2-hydroxybutyrate	0.60	tridecanoate (26)	0.78	
Glycolysis, Gluconeogenesis and Pyruvate Metabolism	glypholate	0.99	Fatty Acid Metabolism (Acyl Carnitine, Medium Chain)	tridecanoate (n3 DPA, 22:5n3)	1.00
	glucose	0.97		tridecanoate (26)	0.76
	glucose 6-phosphate	0.83		tridecanoate (26)	1.13
	2-phosphoglycerate	1.39		tridecanoate (26)	1.00
	3-phosphoglycerate	1.39		tridecanoate (26)	0.76
	phosphoenolpyruvate (PEP)	1.89		tridecanoate (26)	1.13
Glycogen Metabolism	pyruvate	0.81	Fatty Acid Metabolism (Acyl Carnitine, Monounsaturated)	tridecanoate (26)	1.00
	lactate	0.97		tridecanoate (26)	0.76
	malonate	0.87		tridecanoate (26)	1.13
	malonate	0.89		tridecanoate (26)	1.00
	malonate	0.85		tridecanoate (26)	0.76
	malonate	1.11		tridecanoate (26)	1.13
TCA cycle	alpha-ketoglutarate	1.01	Fatty Acid Metabolism (Acyl Carnitine, Polyunsaturated)	tridecanoate (26)	1.00
	2-hydroxybutyrate	0.60		tridecanoate (26)	0.76
Ketone Bodies	3-hydroxybutyrate (3HB)	0.96		tridecanoate (26)	1.13
	nicotinamide	1.03		tridecanoate (26)	1.00
Nicotinate and Nicotinamide Metabolism	NMN	1.06		tridecanoate (26)	0.76
	nicotinamide riboside	0.97		tridecanoate (26)	1.13
	NAD+	1.22	tridecanoate (26)	1.00	
			tridecanoate (26)	0.76	

Furthermore, RNA sequencing was performed (Figure 5A), and enrichment analysis

**Figure 6.** Metabolomic studies performed on hearts from female normal chow-fed hER $\alpha$ <sup>KD</sup> vs. control (n=6/genotype) 4 weeks after Esr1 deletion. Alterations in methionine, pyruvate, and medium and long chain fatty acyl carnitine metabolism. Colored cells are significant  $P < 0.05$ , red  $\uparrow$  metabolites, green  $\downarrow$ . \*,  $P < 0.05$ .

showed beta-hydroxybutyrate dehydrogenase (Bdh1) as the top upregulated gene in hER $\alpha$ <sup>KD</sup> female mice. The encoded protein catalyzes the conversion of acetoacetate and 3-hydroxybutyrate, the two major ketone bodies produced during fatty acid metabolism. Pathway analysis of top enrichment terms for genes were associated with: ATP synthesis, NADH dehydrogenase complex assembly, mitochondrial complex 1 activity, respiratory chain complex assembly, and purine ribonucleotide (Figure 7).

## Discussion

Systolic heart failure, or heart failure with a reduced ejection fraction (HFrEF) is characterized by a left ventricular ejection fraction of 45% or less. Interestingly, the incidence of HFrEF

is more common among men across all ages and accounts for more than half of all heart failure patients. 17beta-esterdiol (E<sub>2</sub>) is the most abundant estrogen in

GO_Biological_Process	GO_TERM	GO_Reference	Actual	Expected	Fold_Enrichment	P-Value	FDR
ATP synthesis coupled proton transport	GO:0015986	19	6	0.26	23.07	8.23E-07	6.48E-04
energy coupled proton transport, down electrochemical gradient	GO:0015985	19	6	0.26	23.07	8.23E-07	6.17E-04
NADH dehydrogenase complex assembly	GO:0010257	49	12	0.67	17.89	2.85E-11	1.12E-07
mitochondrial respiratory chain complex I assembly	GO:0032981	49	12	0.67	17.89	2.85E-11	8.99E-08
protein insertion into mitochondrial membrane	GO:0051204	17	4	0.23	17.19	1.63E-04	3.61E-02
mitochondrial respiratory chain complex assembly	GO:0033108	84	18	1.15	15.65	2.19E-15	3.45E-11
ATP biosynthetic process	GO:0006754	33	7	0.45	15.50	9.72E-07	6.96E-04
mitochondrial ATP synthesis coupled electron transport	GO:0042775	51	9	0.70	12.89	1.07E-07	1.53E-04
oxidative phosphorylation	GO:0006119	73	12	1.00	12.01	1.62E-09	4.24E-06
ATP synthesis coupled electron transport	GO:0042773	55	9	0.75	11.95	1.90E-07	2.14E-04

**Figure 7 Bioinformatic** analyses of RNA sequencing performed on hearts harvested from female, normal chow fed hER $\alpha$ <sup>KD</sup> vs. control (n=6/genotype) 4 weeks after Esr1 deletion. GO analysis reflecting pathways of differentially expressed genes include many mitochondrial-related terms (mitochondrial respiratory chain complex assembly, ATP synthesis, and complex 1 assembly, NADH dehydrogenase complex assembly).

circulation and in post-menopausal women E<sub>2</sub> levels are inversely associated with CVD events<sup>26</sup>. The presence of this sexual dimorphism suggests one potential cardioprotective role for E<sub>2</sub> and ER $\alpha$ . Our functional analysis by echocardiography in hER $\alpha$ <sup>KD</sup> female mice provide further evidence to support this theory. By reducing the expression level of ER $\alpha$  we were able to show a progressive reduction in both left ventricular fractional shortening and left ventricular ejection fraction, with reductions occurring two weeks after gene deletion, reaching significance by week four. These findings confirm previous studies, in which OVX female mice with transverse aortic constriction (TAC) induced HF treated with an ER $\alpha$  agonist, showed smaller reductions in ejection fraction and improved systolic function over a 9-week period<sup>26, 47-48</sup>. Furthermore, histological studies of cardiac tissue

from that same study showed groups treated with the ER $\alpha$  agonist to have a significantly lower fibrosis score<sup>48</sup>. Our work supports those findings as our hER $\alpha$ <sup>KD</sup> model showed significant increases in fibrotic area as compared to controls. Cardiac fibrosis is a well-recognized cause of morbidity and mortality, as it disrupts the coordination of cardiomyocyte excitation and contraction coupling in all phases of contraction leading to a diminished systolic and diastolic function<sup>49,50</sup>. Fibrotic infiltration of cardiac tissue is a process of pathological extra-cellular matrix remodeling, leading to abnormalities in matrix composition and quality. In the case of IRI remodeling can be a preventative wound healing mechanism, but when in excess leads to tissue stiffening and impaired cardiac function. Furthermore, mRNA expression levels of IL-6 and TNF- $\alpha$  in whole heart tissue of the female hER $\alpha$ <sup>KD</sup> were elevated compared to controls. Molecular signals induced by acute injury or chronic stress induce the sequential enlistment of monocytes and macrophages, which can produce pro-inflammatory arbiters like IL-6 and TNF- $\alpha$  and work to infiltrate and repair damaged tissue. Future work will be done to identify whether this cell types are elevated in cardiomyocytes of the hER $\alpha$ <sup>KD</sup> mouse model<sup>49-51</sup>.

In healthy hearts colocalization of ER $\alpha$  with beta-catenin confer structural stability at the intercalated discs of cardiomyocytes. A loss in colocalization could be the trigger for an inflammatory response at the intercalated discs leading collagen infiltration and the progression of HF or other dilated cardiomyopathies. Mahmoodzadeh et al. showed that in human subjects with HF expression levels of ER $\alpha$  are altered in both males and females and end stage heart failure patients have been shown to have a 1.8-fold increase in mRNA expression of ER $\alpha$ . This would further implicate ER $\alpha$  as a cardioprotective agent<sup>52</sup>.

Exhaustive studies of cardiac mitochondria have convincingly established their dysregulation as a molecular symptom of cardiovascular diseases like arrhythmias, myocardial ischemia, and heart failure. Mitochondria are highly dynamic organelles with two opposing highly regulated processes, fusion (joining) and fission (division)<sup>41</sup>. Fission-fusion dynamics allow living cells to modulate cell architecture and metabolism as they respond to environmental stimuli and perturbations<sup>53-56</sup>. It has been suggested that while the upregulation of fusion machinery is cardioprotective, increases in fission factors triggers mitochondrial fragmentation leading to cell death which can be detrimental to the heart<sup>55-56</sup>. In the context of reduced ER $\alpha$  in cardiomyocytes, our hER $\alpha$ <sup>KD</sup> mice show a significant and deleterious shift in mitochondrial architecture. Electron micrograph images showed significant reductions in percent area fraction and number of cristae within the mitochondria. Moreover, western blot analysis showed marked changes in fission and apoptosis machinery (Drp1, Fis1, p62). These data confirm previous findings by our lab that *Esr1* exerts a strong regulatory control over mitochondrial form. Dynamin related protein-1 (Drp1) is a large GTPase protein that assists in fission events by spiraling around the outer mitochondrial membrane to facilitate the scission of the plasma membrane<sup>57-59</sup>. Mitochondrial fission protein-1 (Fis1) is a small transmembrane protein anchored to the outer mitochondrial membrane (OMM) that is thought to be involved in the recruitment of cytosolic Drp1 to the OMM<sup>59</sup>. Previous studies have shown that mice with a cardiac specific deletion of Drp1 exhibited a dysregulated mitochondrial network and subsequently developed a left ventricular dysfunction and died within 13 weeks<sup>60</sup>. These data suggest that ER $\alpha$  may be a significant player in the coordination fission

machinery, mitochondrial health and indirectly correlated to the onset and progression of HF.

To maintain the constant work of the heart, mitochondria within cardiomyocytes must produce amounts ATP large enough to meet demand<sup>61</sup>. As discussed, heart failure is accompanied by deleterious alterations in mitochondrial function specifically ATP production. Because EM images of hER $\alpha$ <sup>KD</sup> mice showed marked reductions in cristae numbers and area, and previous studies by our lab have shown that Drp1 is critical for cristae formation and the assembly of the electron transport chain (ETC) we suspected some sort of ETC dysfunction. Surprisingly, we did not see a significant reduction in oxidative phosphorylation, but we did see a reduction in complex I activity. These findings were reaffirmed by RNAseq data which indicated top enrichment score genes to be associated with ATP synthesis, NADH dehydrogenase complex assembly, mitochondrial complex 1, respiratory chain complex assembly, and purine ribonucleotide. Future work interrogating why complex I activity is decreased but not oxygen consumption rate is required.

The coordination of fatty acid metabolism from circulation vs. endogenous stores (triacylglycerol, TAG) and the regulation of their fate has reemerged as an active area of investigation due to the relevance of metabolism in the etiology of HF<sup>46</sup>. Interestingly, women have higher myocardial TAG and TAG turnover rates compared with men, and TAG content and turnover are important predictors of pathology in the failing heart, as impairment of turnover is associated with increased lipotoxic acyl intermediates, hypertrophy, and inflammation. The sex-specific mechanisms regulating these differences in fatty acid metabolism in cardiomyocytes remain inadequately defined. To

address this gap in research we performed metabolomics studies on hER $\alpha$ <sup>KD</sup> and control mice. hER $\alpha$ <sup>KD</sup> showed a remarkable metabolic remodeling. As seen by significant changes in methionine, pyruvate, and medium and long chain fatty acyl carnitine metabolism. This may indicate a switch in fuel substrate utilization which has been shown to be a characteristic of cardiomyocytes under failing conditions.

### **Conclusion**

Gender is increasingly recognized as a major factor in the outcomes of patients with cardiovascular diseases (CVD). Here we have shown that the estrogen receptor alpha does in fact direct a number of cardioprotective functions. Our work implicates ER $\alpha$  as a modulator both cardiac form and function. Functionally, our *Esr1* knock-down model showed a progressive reduction of left ventricular ejection fraction (LVEF), left ventricular fractional shortening (LVFS), and an increase in left ventricular internal diameter during systole (LVIDs) reaching significance at 4 weeks after gene deletion. Each of these functional readouts is indicative of cardiomyopathy, specifically heart failure. Furthermore, we showed hER $\alpha$ <sup>KD</sup> female mice incurred a marked increase in fibrotic area, as well as increases in inflammatory markers within the heart. This increase in fibrotic area may be the cause of the reduced ejection fraction, because of reduced cardiac contractility and increased myocyte rigidity. Previous work has implicated mitochondrial disequilibrium as a molecular signature of heart failure in both men and women. Interestingly, we have shown that the loss of *Esr1* in cardiomyocytes leads to dramatic changes in inner and outer mitochondrial architecture. With a pathologic loss of cristae density, increases in apoptotic, fission, and autophagic factors, we also see a reduction in electron transport chain activity, specifically at complex I. Finally, we have begun to

uncover what shifts in cardiomyocyte substrate metabolism occur in HF models because of E<sub>2</sub> mediated action through ER $\alpha$ . To our knowledge, most published studies have been conducted on whole body *Esr1* knock out mice, where non-cardiac cells can contribute to deleterious heart phenotypes, as this mouse model is confounded by obesity, insulin resistance, hyperglycemia, elevated PAI-1, immune cell inflammation, and endothelial dysfunction. Our conditional and cardiac specific model of *Esr1* deletion allow us to study the early defects that arise in the cardiomyocyte as a consequence of ER $\alpha$  inactivation. We hope that future studies will continue our work, furthering our understanding about how E<sub>2</sub> selectively works through ER $\alpha$  which will one day be vital for the development of effective therapeutic strategies to prevent HF and other cardiomyopathies in both men and women.



## References

1. Levenson, J. W., Skerrett, P. J., & Gaziano, J. M. (2002). Reducing the global burden of cardiovascular disease: the role of risk factors. *Preventive cardiology*, 5(4), 188-199.
2. World Health Organization. (1999). *The world health report: 1999: making a difference*. World Health Organization.
3. Lopez, A. D., & Murray, C. C. (1998). The global burden of disease, 1990–2020. *Nature medicine*, 4(11), 1241-1243.
4. Mc Namara, K., Alzubaidi, H., and Jackson, J. K. (2019) Cardiovascular disease as a leading cause of death: how are pharmacists getting involved? *Integr Pharm Res Pract* 8, 1-11
5. Virani, S. S., Alonso, A., Benjamin, E. J., Bittencourt, M. S., Callaway, C. W., Carson, A. P., Chamberlain, A. M., Chang, A. R., Cheng, S., Delling, F. N., Djousse, L., Elkind, M. S. V., Ferguson, J. F., Fornage, M., Khan, S. S., Kissela, B. M., Knutson, K. L., Kwan, T. W., Lackland, D. T., Lewis, T. T., Lichtman, J. H., Longenecker, C. T., Loop, M. S., Lutsey, P. L., Martin, S. S., Matsushita, K., Moran, A. E., Mussolino, M. E., Perak, A. M., Rosamond, W. D., Roth, G. A., Sampson, U. K. A., Satou, G. M., Schroeder, E. B., Shah, S. H., Shay, C. M., Spartano, N. L., Stokes, A., Tirschwell, D. L., VanWagner, L. B., Tsao, C. W., American Heart Association Council on, E., Prevention Statistics, C., and Stroke Statistics, S. (2020) Heart Disease and Stroke Statistics-2020 Update: A Report From the American Heart Association. *Circulation* 141, e139-e596

6. Khan, M. A., Hashim, M. J., Mustafa, H., Baniyas, M. Y., Al Suwaidi, S., AlKatheeri, R., Alblooshi, F. M. K., Almatrooshi, M., Alzaabi, M. E. H., Al Darmaki, R. S., and Lootah, S. (2020) Global Epidemiology of Ischemic Heart Disease: Results from the Global Burden of Disease Study. *Cureus* **12**, e9349
7. Voigt, J., John, M. S., Taylor, A., Krucoff, M., Reynolds, M. R., & Michael Gibson, C. (2014). A reevaluation of the costs of heart failure and its implications for allocation of health resources in the United States. *Clinical cardiology*, *37*(5), 312-321.
8. Travessa, A. M. R., & de Menezes Falcao, L. F. (2016). Treatment of Heart Failure With Reduced Ejection Fraction—Recent Developments. *American Journal of Therapeutics*, *23*(2), e531-e549.
9. Leske, M. C., Wu, S. Y., Hennis, A., Honkanen, R., Nemesure, B., & BESs Study Group. (2008). Risk factors for incident open-angle glaucoma: the Barbados Eye Studies. *Ophthalmology*, *115*(1), 85-93.
10. Lam CSP, Arnott C, Beale AL, Chandramouli C, Hilfiker-Kleiner D, Kaye DM, Ky B, Santema BT, Sliwa K, Voors AA. Sex differences in heart failure. *Eur Heart J*. 2019;40(47):3859-68c. doi: 10.1093/eurheartj/ehz835. PubMed PMID: 31800034.
11. Lala A, Tayal U, Hamo CE, Youmans Q, Al-Khatib SM, Bozkurt B, Davis MB, Januzzi J, Mentz R, Sauer A, Walsh MN, Yancy C, Gulati M. Sex Differences in Heart Failure. *J Card Fail*. 2022;28(3):477-98. Epub 20211110. doi: 10.1016/j.cardfail.2021.10.006. PubMed PMID: 34774749.

12. Mentzer G, Hsich EM. Heart Failure with Reduced Ejection Fraction in Women: Epidemiology, Outcomes, and Treatment. *Heart Fail Clin.* 2019;15(1):19-27. Epub 20181024. doi: 10.1016/j.hfc.2018.08.003. PubMed PMID: 30449377; PMCID: PMC6298793.
13. Anderson GL, Limacher M, Assaf AR, Bassford T, Beresford SA, Black H, Bonds D, Brunner R, Brzyski R, Caan B, Chlebowski R, Curb D, Gass M, Hays J, Heiss G, Hendrix S, Howard BV, Hsia J, Hubbell A, Jackson R, Johnson KC, Judd H, Kotchen JM, Kuller L, LaCroix AZ, Lane D, Langer RD, Lasser N, Lewis CE, Manson J, Margolis K, Ockene J, O'Sullivan MJ, Phillips L, Prentice RL, Ritenbaugh C, Robbins J, Rossouw JE, Sarto G, Stefanick ML, Van Horn L, Wactawski-Wende J, Wallace R, Wassertheil-Smoller S, Women's Health Initiative Steering C. Effects of conjugated equine estrogen in postmenopausal women with hysterectomy: the Women's Health Initiative randomized controlled trial. *JAMA.* 2004;291(14):1701-12. doi: 10.1001/jama.291.14.1701. PubMed PMID: 15082697.
14. Heiss G, Wallace R, Anderson GL, Aragaki A, Beresford SA, Brzyski R, Chlebowski RT, Gass M, LaCroix A, Manson JE, Prentice RL, Rossouw J, Stefanick ML, Investigators WHI. Health risks and benefits 3 years after stopping randomized treatment with estrogen and progestin. *JAMA.*
15. Prentice RL, Aragaki AK, Chlebowski RT, Rossouw JE, Anderson GL, Stefanick ML, Wactawski-Wende J, Kuller LH, Wallace R, Johnson KC, Shadyab AH, Gass M, Manson JE. Randomized Trial Evaluation of the Benefits and Risks of Menopausal Hormone Therapy Among Women 50-59 Years of Age. *Am J*

- Epidemiol. 2021;190(3):365-75. doi: 10.1093/aje/kwaa210. PubMed PMID: 33025002; PMCID: PMC8086238.
16. Miller VM, Naftolin F, Asthana S, Black DM, Brinton EA, Budoff MJ, Cedars MI, Dowling NM, Gleason CE, Hodis HN, Jayachandran M, Kantarci K, Lobo RA, Manson JE, Pal L, Santoro NF, Taylor HS, Harman SM. The Kronos Early Estrogen Prevention Study (KEEPS): what have we learned? *Menopause*. 2019;26(9):1071-84. doi: 10.1097/GME.0000000000001326. PubMed PMID: 31453973; PMCID: PMC6738629.
17. Kolar V, Vastrad B, Vastrad C, Kotturshetti S, Tengli A. Identification of candidate biomarkers and therapeutic agents for heart failure by bioinformatics analysis. *BMC Cardiovasc Disord*. 2021;21(1):329. Epub 20210704. doi: 10.1186/s12872-021-02146-8. PubMed PMID: 34218797; PMCID: PMC8256614.
18. Dosi, R., Bhatt, N., Shah, P., and Patell, R. (2014) Cardiovascular disease and menopause. *J Clin Diagn Res* **8**, 62-64
19. Iorga, A., Cunningham, C. M., Moazeni, S., Ruffenach, G., Umar, S., and Eghbali, M. (2017) The protective role of estrogen and estrogen receptors in cardiovascular disease and the controversial use of estrogen therapy. *Biol Sex Differ* **8**, 33
20. Sickinghe, A. A., Korporaal, S. J. A., den Ruijter, H. M., and Kessler, E. L. (2019) Estrogen Contributions to Microvascular Dysfunction Evolving to Heart Failure With Preserved Ejection Fraction. *Front Endocrinol (Lausanne)* **10**, 442
21. Westphal, C., Schubert, C., Prella, K., Penkalla, A., Fliegner, D., Petrov, G., and Regitz-Zagrosek, V. (2012) Effects of estrogen, an ERalpha agonist and

- raloxifene on pressure overload induced cardiac hypertrophy. *PLoS One* **7**, e50802
22. Wang, M., Crisostomo, P., Wairiuko, G. M., and Meldrum, D. R. (2006) Estrogen receptor-alpha mediates acute myocardial protection in females. *Am J Physiol Heart Circ Physiol* **290**, H2204-2209
23. Murphy, E., and Steenbergen, C. (2007) Gender-based differences in mechanisms of protection in myocardial ischemia-reperfusion injury. *Cardiovasc Res* **75**, 478-486
24. Mahmoodzadeh, S., Eder, S., Nordmeyer, J., Ehler, E., Huber, O., Martus, P., Weiske, J., Pregla, R., Hetzer, R., and Regitz-Zagrosek, V. (2006) Estrogen receptor alpha up-regulation and redistribution in human heart failure. *FASEB J* **20**, 926-934
25. Hevener, A. L., Ribas, V., Moore, T. M., and Zhou, Z. (2020) ERalpha in the Control of Mitochondrial Function and Metabolic Health. *Trends Mol Med*
26. Aryan, L., Younessi, D., Zargari, M., Banerjee, S., Agopian, J., Rahman, S., Borna, R., Ruffenach, G., Umar, S., & Eghbali, M. (2020). The Role of Estrogen Receptors in Cardiovascular Disease. *International journal of molecular sciences*, 21(12), 4314. <https://doi.org/10.3390/ijms21124314>
27. Marino, M., Galluzzo, P., & Ascenzi, P. (2006). Estrogen signaling multiple pathways to impact gene transcription. *Current genomics*, 7(8), 497-508.
28. Borlaug, B. A. (2014). The pathophysiology of heart failure with preserved ejection fraction. *Nature Reviews Cardiology*, 11(9), 507-515.

29. Zile, M. R., Gaasch, W. H., Carroll, J. D., Feldman, M. D., Aurigemma, G. P., Schaer, G. L., ... & Liebson, P. R. (2001). Heart failure with a normal ejection fraction: is measurement of diastolic function necessary to make the diagnosis of diastolic heart failure?. *Circulation*, *104*(7), 779-782.
30. Zile, M. R., Gottdiener, J. S., Hetzel, S. J., McMurray, J. J., Komajda, M., McKelvie, R., ... & Carson, P. E. (2011). Prevalence and significance of alterations in cardiac structure and function in patients with heart failure and a preserved ejection fraction. *Circulation*, *124*(23), 2491-2501.
31. van Heerebeek, L., Borbély, A., Niessen, H. W., Bronzwaer, J. G., van der Velden, J., Stienen, G. J., ... & Paulus, W. J. (2006). Myocardial structure and function differ in systolic and diastolic heart failure. *Circulation*, *113*(16), 1966-1973.
32. Borbély, A., Van Der Velden, J., Papp, Z., Bronzwaer, J. G., Edes, I., Stienen, G. J., & Paulus, W. J. (2005). Cardiomyocyte stiffness in diastolic heart failure. *Circulation*, *111*(6), 774-781.
33. Bertero E, Maack C. Metabolic remodelling in heart failure. *Nat Rev Cardiol*. 2018;15(8):457-70. doi: 10.1038/s41569-018-0044-6. PubMed PMID: 29915254.
34. Mandsager K, Harb S, Cremer P, Phelan D, Nissen SE, Jaber W. Association of Cardiorespiratory Fitness With Long-term Mortality Among Adults Undergoing Exercise Treadmill Testing. *JAMA Netw Open*. 2018;1(6):e183605. Epub 20181005. doi: 10.1001/jamanetworkopen.2018.3605. PubMed PMID: 30646252; PMCID: PMC6324439.

35. Shen K, Pender CL, Bar-Ziv R, Zhang H, Wickham K, Willey E, Durieux J, Ahmad Q, Dillin A. Mitochondria as Cellular and Organismal Signaling Hubs. *Annu Rev Cell Dev Biol.* 2022. Epub 20220708.
36. Lopaschuk GD, Karwi QG, Ho KL, Pherwani S, Ketema EB. Ketone metabolism in the failing heart. *Biochim Biophys Acta Mol Cell Biol Lipids.* 2020;1865(12):158813. Epub 20200910. doi: 10.1016/j.bbalip.2020.158813. PubMed PMID: 32920139.
37. Karwi QG, Biswas D, Pulinilkunnil T, Lopaschuk GD. Myocardial Ketones Metabolism in Heart Failure. *J Card Fail.* 2020;26(11):998-1005. Epub 20200519. doi: 10.1016/j.cardfail.2020.04.005. PubMed PMID: 32442517.
38. Ho KL, Zhang L, Wagg C, Al Batran R, Gopal K, Levasseur J, Leone T, Dyck JRB, Ussher JR, Muoio DM, Kelly DP, Lopaschuk GD. Increased ketone body oxidation provides additional energy for the failing heart without improving cardiac efficiency. *Cardiovasc Res.* 2019;115(11):1606-16. doi: 10.1093/cvr/cvz045. PubMed PMID: 30778524; PMCID: PMC6704391.
39. Ho KL, Karwi QG, Wagg C, Zhang L, Vo K, Altamimi T, Uddin GM, Ussher JR, Lopaschuk GD. Ketones can become the major fuel source for the heart but do not increase cardiac efficiency. *Cardiovasc Res.* 2021;117(4):1178-87. doi: 10.1093/cvr/cvaa143. PubMed PMID: 32402081; PMCID: PMC7982999.
40. Pernas L, Scorrano L. Mito-Morphosis: Mitochondrial Fusion, Fission, and Cristae Remodeling as Key Mediators of Cellular Function. *Annu Rev Physiol.* 2016;78:505-31. Epub 20151119. doi: 10.1146/annurev-physiol-021115-105011. PubMed PMID: 26667075.

41. Marín-García, J., & Akhmedov, A. T. (2016). Mitochondrial dynamics and cell death in heart failure. *Heart failure reviews*, 21(2), 123-136.
42. Tolkovsky, A. M. (2009). Mitophagy. *Biochimica et Biophysica Acta (BBA)-Molecular Cell Research*, 1793(9), 1508-1515.
43. Gomes, L. C., & Scorrano, L. (2013). Mitochondrial morphology in mitophagy and macroautophagy. *Biochimica et Biophysica Acta (BBA)-Molecular Cell Research*, 1833(1), 205-212.
44. Sohal, D. S., Nghiem, M., Crackower, M. A., Witt, S. A., Kimball, T. R., Tymitz, K. M., ... & Molkenin, J. D. (2001). Temporally regulated and tissue-specific gene manipulations in the adult and embryonic heart using a tamoxifen-inducible Cre protein. *Circulation research*, 89(1), 20-25.
45. Acin-Perez R, Benador IY, Petcherski A, Veliova M, Benavides GA, Lagarrigue S, Caudal A, Vergnes L, Murphy AN, Karamanlidis G, Tian R, Reue K, Wanagat J, Sacks H, Amati F, Darley-Usmar VM, Liesa M, Divakaruni AS, Stiles L, Shirihai OS. A novel approach to measure mitochondrial respiration in frozen biological samples. *EMBO J*. 2020;39(13):e104073. Epub 20200520. doi: 10.15252/emboj.2019104073. PubMed PMID: 32432379; PMCID: PMC7327496.
46. Lahey R, Wang X, Carley AN, Lewandowski ED. Dietary fat supply to failing hearts determines dynamic lipid signaling for nuclear receptor activation and oxidation of stored triglyceride. *Circulation*. 2014;130(20):1790-9. Epub 20140929. doi: 10.1161/CIRCULATIONAHA.114.011687. PubMed PMID: 25266948; PMCID: PMC4229424.



47. Sickinghe, A. A., Korporaal, S. J., Den Ruijter, H. M., & Kessler, E. L. (2019). Estrogen contributions to microvascular dysfunction evolving to heart failure with preserved ejection fraction. *Frontiers in Endocrinology*, *10*, 442.
48. Westphal, C., Schubert, C., Prella, K., Penkalla, A., Fliegner, D., Petrov, G., & Regitz-Zagrosek, V. (2012). Effects of estrogen, an ER $\alpha$  agonist and raloxifene on pressure overload induced cardiac hypertrophy. *PloS one*, *7*(12), e50802.
49. Kong, P., Christia, P., & Frangogiannis, N. G. (2014). The pathogenesis of cardiac fibrosis. *Cellular and molecular life sciences*, *71*(4), 549-574.
50. Janicki, J. S., & Brower, G. L. (2002). The role of myocardial fibrillar collagen in ventricular remodeling and function. *Journal of cardiac failure*, *8*(6), S319-S325.
51. Nahrendorf M, Swirski FK, Aikawa E, Stangenberg L, Wurdinger T, Figueiredo JL, Libby P, Weissleder R, Pittet MJ (2007) The healing myocardium sequentially mobilizes two monocyte subsets with divergent and complementary functions. *J Exp Med* 204:3037–3047
52. Mahmoodzadeh, S., Eder, S., Nordmeyer, J., Ehler, E., Huber, O., Martus, P., ... & Regitz-Zagrosek, V. (2006). Estrogen receptor alpha up-regulation and redistribution in human heart failure. *The FASEB Journal*, *20*(7), 926-934.
53. Liesa, M., Palacín, M., & Zorzano, A. (2009). Mitochondrial dynamics in mammalian health and disease. *Physiological reviews*, *89*(3), 799-845.
54. Westermann, B. (2010). Mitochondrial fusion and fission in cell life and death. *Nature reviews Molecular cell biology*, *11*(12), 872-884.
55. Youle, R. J., & Van Der Bliek, A. M. (2012). Mitochondrial fission, fusion, and stress. *Science*, *337*(6098), 1062-1065.

56. Friedman, J. R., & Nunnari, J. (2014). Mitochondrial form and function. *Nature*, *505*(7483), 335-343.
57. Fonseca, T. B., Sánchez-Guerrero, Á., Milosevic, I., & Raimundo, N. (2019). Mitochondrial fission requires DRP1 but not dynamins. *Nature*, *570*(7761), E34-E42.
58. Otera, H., Ishihara, N., & Mihara, K. (2013). New insights into the function and regulation of mitochondrial fission. *Biochimica et Biophysica Acta (BBA)-Molecular Cell Research*, *1833*(5), 1256-1268.
59. Elgass, K., Pakay, J., Ryan, M. T., & Palmer, C. S. (2013). Recent advances into the understanding of mitochondrial fission. *Biochimica et Biophysica Acta (BBA)-Molecular Cell Research*, *1833*(1), 150-161.
60. Tondera, D., Grandemange, S., Jourdain, A., Karbowski, M., Mattenberger, Y., Herzig, S., ... & Martinou, J. C. (2009). SLP-2 is required for stress-induced mitochondrial hyperfusion. *The EMBO journal*, *28*(11), 1589-1600.
61. Zhou B, Tian R. Mitochondrial dysfunction in pathophysiology of heart failure. *J Clin Invest*. 2018;128(9):3716-26. Epub 20180820. doi: 10.1172/JCI120849. PubMed PMID: 30124471; PMCID: PMC6118589.